EPJ Web of Conferences **181**, 01037 (2018) https://doi.org/10.1051/epjconf/201818101037
EXA2017

AEḡIS latest results

F. Guatieri[1,2], *S.* Aghion[3,5], *C.* Amsler[6], *G.* Angela[5], *G.* Bonomi[7,8], *R.S.* Brusa[1,2], *M.* Caccia[4,9], *R.* Caravita[10,11], *F.* Castelli[4,13], *G.* Cerchiari[14], *D.* Comparat[15], *G.* Consolati[3,4], *A.* Demetrio[16], *L.* Di Noto[10,11], *M.* Doser[12], *C.* Evans[3,4], *M.* Fanì[10,11,12], *R.* Ferragut[3,4], *J.* Fesel[12], *A.* Fontana[8], *S.* Gerber[12], *M.* Giammarchi[4], *A.* Gligorova[17], *S.* Haider[12], *A.* Hinterberger[12], *H.* Holmestad[19], *A.* Kellerbauer[14], *D.* Krasnický[10,11], *V.* Lagomarsino[10,11], *P.* Lansonneur[20], *P.* Lebrun[20], *C.* Malbrunot[12,6], *S.* Mariazzi[23], *V.* Matveev[21,22], *Z.* Mazzotta[4,13], *S.R.* Müller[16], *G.* Nebbia[23], *P.* Nedelec[20], *M.* Oberthaler[16], *N.* Pacifico[17], *D.* Pagano[7,8], *L.* Penasa[1,2], *V.* Petracek[18], *F.* Prelz[4], *M.* Prevedelli[24], *B.* Rienaecker[12], *J.* Robert[15], *O.M.* Rhne.[19], *A.* Rotondi[8,25], *M.* Sacerdoti[4,13], *H.* Sandaker[19], *R.* Santoro[4,9], *M.* Simon[6], *L.* Smestad[12,27], *F.* Sorrentino[10,11], *G.* Testera[11], *I.C.* Tietje[12], *E.* Widmann[6], *P.* Yzombard[14], *C.* Zimmer[12,14,16], *J.* Zmeskal[6], *N.* Zurlo[8,28]

[1]Department of Physics, University of Trento
[2]TIFPA/INFN Trento
[3]Politecnico of Milano
[4]Istituto Nazionale di Fisica Nucleare, Sezione di Milano
[5]Laboratory for High Energy Physics, Albert Einstein Center for Fundamental Physics, University of Bern
[6]Stefan Meyer Institute for Subatomic Physics, Austrian Academy of Sciences
[7]Department of Mechanical and Industrial Engineering, University of Brescia
[8]INFN Pavia
[9]Department of Science, University of Insubria
[10]Department of Physics, University of Genova
[11]INFN Genova
[12]Physics Department, CERN
[13]Department of Physics, Università degli Studi di Milano
[14]Max Planck Institute for Nuclear Physics
[15]Laboratoire Aimé Cotton, Université Paris-Sud, ENS Cachan, CNRS
[16]Kirchhoff-Institute for Physics, Heidelberg University
[17]Institute of Physics and Technology, University of Bergen
[18]Czech Technical University, Prague
[19]Department of Physics, University of Oslo
[20]Institute of Nuclear Physics, CNRS/IN2p3
[21]Institute for Nuclear Research of the Russian Academy of Science, Moscow
[22]Joint Institute for Nuclear Research, Dubna
[23]INFN Padova
[24]University of Bologna
[25]Department of Physics, University of Pavia
[26]Department of Physics "Ettore Pancini" University of Napoli Federico II
[27]The Research Council of Norway
[28]Department of Civil Engineering, University of Brescia

Abstract. The validity of the Weak Equivalence Principle (WEP) as predicted by General Relativity has been tested up to astounding precision using ordinary

matter. The lack hitherto of a stable source of a probe being at the same time electrically neutral, cold and stable enough to be measured has prevented high-accuracy testing of the WEP on anti-matter. The AE$\bar{g}$IS (Antimatter Experiment: Gravity, Interferometry, Spectroscopy) experiment located at CERN's AD (Antiproton Decelerator) facility aims at producing such a probe in the form of a pulsed beam of cold anti-hydrogen, and at measuring by means of a moiré deflectometer the gravitational force that Earth's mass exerts on it. Low temperature and abundance of the $\bar{H}$ are paramount to attain a high precision measurement. A technique employing a charge-exchange reaction between antiprotons coming from the AD and excited positronium atoms is being developed at AE$\bar{g}$IS and will be presented hereafter, alongside an overview of the experimental apparatus and the current status of the experiment

1 Introduction

Despite strong and electroweak matter-antimatter interactions being widely studied in the last 85 years, as of today nobody has been able to observe antimatter interact through gravity. Most current theories predict antimatter and matter to be identically subject to the gravitational force; one of the most compelling reasons for this symmetry resides in the fact that it lies at the foundation of the general theory of relativity, as stated by the weak equivalence principle. The ratio between gravitational mass m_g and inertial mass m_i for ordinary matter has been determined to be constant up to more that 0.21 parts per trillion [1], whereas when comparing matter and antimatter probes as of today we are only able to set an upper limit of $|m_g/m_i| < 75$ [2].

The AE$\bar{g}$IS experiment aims to measure directly the free-fall of an uncharged probe, antihydrogen, and thus to determine the aforementioned ratio to less than a part in 10^2. Gravitational pull will be measured directly by letting an uncollimated beam of cold antihydrogen travel through a moiré deflectometer[3] as shown in figure 1. Both the time of flight Δt through the full deflectometer and the vertical displacement Δt to which the particles were subject will need to be measured. Thanks to the geometry of the deflectometer the gravitational pull can then be determined as:

$$g = 4 \cdot \frac{\Delta y}{\Delta t^2}$$

The time of flight measurement necessitates a pulsed production scheme to provide a suitable start signal, whereas the vertical displacement measurement benefits from low $\bar{\mathrm{H}}$ temperature, the vertical displacement being determined by the axial component of the impinging $\bar{\mathrm{H}}$ velocity.

To meet its demand of pulsed cold $\bar{\mathrm{H}}$, AE$\bar{g}$IS employs the charge exchange production scheme shown in figure 2; it consists in having an antiproton react with a Rydberg excited positronium, producing an antihydrogen and freeing the electron as a result. Positronium production can be performed in short bursts, hence resulting in a pulsed production scheme, moreover employing positronium excited in a high Rydberg state heavily increases the reaction cross-section[4]. Finally the charge reaction transfers less recoil to the emerging $\bar{\mathrm{H}}$ as opposed to the mixing production scheme[5] thus allowing for the production of colder antihydrogen[6].

Production of positronium in AE$\bar{g}$IS is perfomed by implanting a beam of positrons into a nanochanneled silicon chip coated in SiO_2 [7] at an energy comprised between 4 keV and 7 keV. Nanochanneled silicon converts positron into positronium; producing a cloud of cool

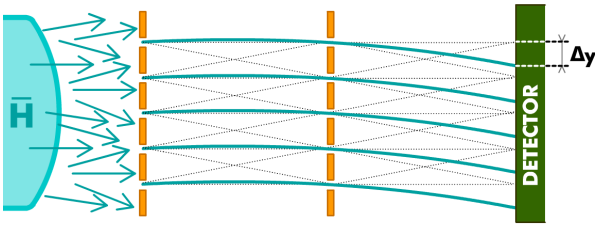

Figure 1. Working principle of a moiré deflectometer. Although the incoming beam is uncollimated, determination of the time-of-flight Δt and vertical displacement Δy of the particles reaching the detector is, thanks to the deflectometer geometry, enough to determine the gravitational pull they underwent in flight.

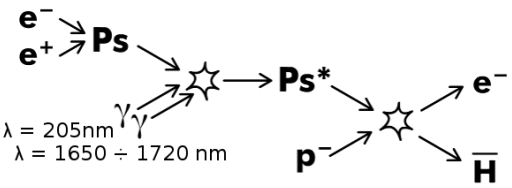

Figure 2. $\bar{\mathrm{H}}$ production through charge exchange process. Antiprotons react with positronium excited into Rydberg states producing an antihydrogen and freeing the electron in the process.

positronium exiting the target with a speed distribution mostly comprised under 10^5m/s with an overall efficiency of about 10%[7][8]. The AE$\bar{\mathrm{g}}$IS positron line, consisting in a ^{22}Na source coupled with a solid Ne moderator[9], Surko-type trap[10] followed by a Malmberg-Penning trap is capable of delivering 20 ns long bunches of $10^7 \div 10^8$ particles. Positronium is produced in-situ with the target placed a few centimeters from the $\bar{\mathrm{p}}$ cloud, and then excited to a Rydberg state by means of two laser pulses shot parallel to the nanochannel plate a few millimeters from the surface[11].

When the cloud of excited positronium intersects the $\bar{\mathrm{p}}$ cloud inside of the production trap the charge exchange reaction takes place and anithydrogen is produced which will then be extracted by means of stark acceleration from the production trap and conveyed onto the deflectometer to perform the actual measurement.

2 Commissioning of the positronium line

As of 2015 the construction of the positron line was finalized[12] and its commissioning and optimization began. To test and optimize the mechanism of conversion of positrons and cooling of positronium by means of nanostructured silica the AE$\bar{\mathrm{g}}$IS experiment features a secondary positron experimental chamber into which the positron beam can be steered instead of being injected into the main traps line. When employed in the seconday positron chamber, the positron beam shots can be further compressed by a buncher from 20 ns to 7 ns. The secondary positron chamber features a sample holder onto which several targets can be loaded and moved onto the beam spot. Alternatively if the sample holder is moved out of

the way of the positron beam, the beam will, instead, impact onto a micro channel plate (MCP) coupled with a phosphor screen. The phosphor screen provides a image of the beam spot that can be acquired through a digital camera placed beyond a viewport. Additionally two $PbWO_4$ scintillating crystals paired with photomultiplier tubes are placed right above and below the target to detect γ rays deriving from positron annihilations in the target or positronium annihilations either in flight or against the chamber walls.

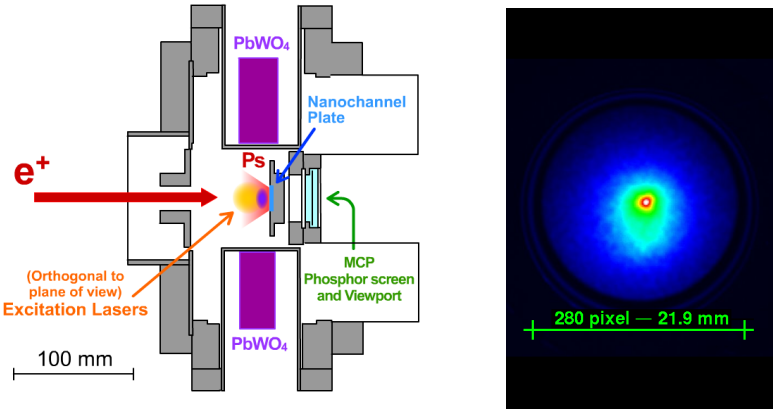

Figure 3. On the left a sectional view of the secondary positron chamber, the laser enters the chamber orthogonal to the section plane. On the right imaging of the positron spot performed with the MCP + Phosphor screen detector; the spot FWHM (defined as the diameter of region with an intensity above half of the peak intensity) measures 2.8 mm.

The alignment and size of the positron beam have been optimized by employing direct imaging of the beam, its temporal profile has been optimized by observing the length of the bursts detected with PbF_2 Čerenkov detectors. If a nanochanneled silica target is placed in the way of the positron beam then the produced positronium can be studied using the Single Shot Positron Annihilation Lifetime Spectroscopy (SSPALS) measurement [13]. An SSPALS spectrum is, in our setup, the shape of the signal profile given by the two $PbWO_4$ detectors which we acquire after digitizing it through a digital oscilloscope. An example of SSPALS spectrum is shown in figure 4. SSPALS spectra of nanochanneled silica targets sport a prompt peak a few tens of nanoseconds long and an exponentially shaped tail which consists of the produced cold positronium being emitted by the target and annihilating in flight. At longer times the SSPALS profile might exceed the exponential decay if enough positronium reaches the chamber walls for its annihilation against them to be detectable over the noise.

The secondary positron chamber allows for direct positronium spectroscopy measurements which, in turn, present the benefit of allowing the commissioning and calibration of the laser apparatus. The AE$\bar{g}$IS apparatus contains three laser sources: a UV laser ($\lambda = 205$ nm) tuned to the $1^3S \rightarrow 3^3P$ transition; a ionization laser ($\lambda = 1064$ nm) which is enough to ionize a positronium previously excited to the 3^3P state and the Rydberg-excitation laser with a tunable wavelength comprised between 1650 and 1720 nm which can excite positronium from the 3^3P state to Rydberg band states from $n = 14$ to $n = 18$.

We were able to employ the secondary positron chamber and the laser apparatus to produce and detect $n = 3$ states of positronium[14] by comparing the area under the SSPALS spectrum in a region adjacent to the main prompt peak when the UV laser was shone onto the positronium cloud and when both the UV and the Ionization laser where shone onto it.

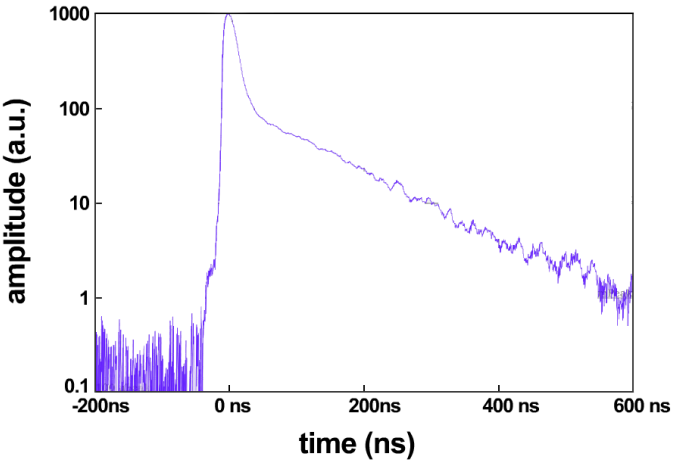

Figure 4. Example of SSPALS spectrum, the logarithmic scale plot shows the exponential decay of the positronium tail in the form of a downward sloping straight line following the prompt peak.

The decrease of the SSPALS spectrum height as consequence of the addition of the ionization laser is an unequivocal indicator of the successful production of $n = 3$ positronium. In the same measurement campaign[14] we were able to demonstrate production of Rydberg states of positronium by shining the UV and Rydberg lasers together and observing the increase of height of the SSPALS spectrum at longer times after the peak, when we expect the excited positronium to annihilate against the chamber walls. Due to its lifetime[15] spanning in the order of microseconds we expect most of Rydberg positronium to reach and annihilate onto the chamber walls. Tuning the frequency of the Rydberg laser shows the Rydberg transitions as variation in the area under the curve at high times (see figure 5).

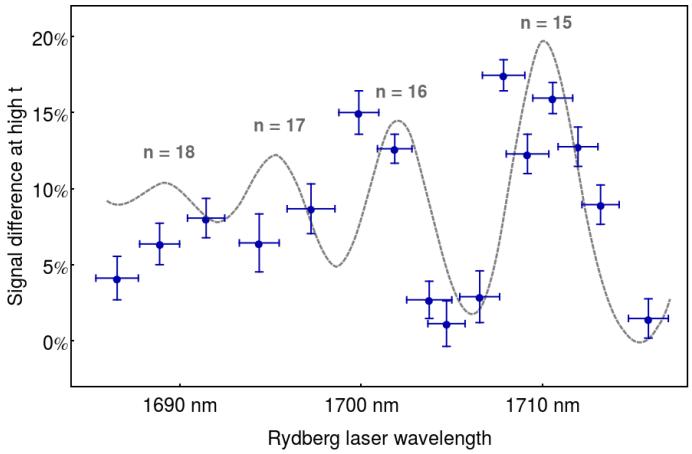

Figure 5. Variation in the SSPALS intensity at long times (> 300 ns from the prompt peak) as a function of the Rydberg laser wavelength, the $n = 15$ peak is visible while the $n = 16$ is hinted

3 Recent results

As of now we are capable of reliably moderate and capture bunches produced by the AD apparatus with an overall efficiency of 1%. The mean life of antiprotons inside of the AE$\bar{g}$IS trap system exceeds 10^3s. Shots captured from AD are then compressed (efficiency 45%) and transferred (efficiency >80%) into the production trap resulting in a plasma of $1.4 \cdot 10^5$ $\bar{p}$ and a radius of 0.5 mm. We are capable of stacking up to three AD shots resulting in a total accumulation of $4 \cdot 10^5$ $\bar{p}$.

Due to a novel upgrade to the positron transfer line we are able as of today to inject positrons directly from the positron line across the whole trap lineup onto the nanochanneled silica converter placed on top of the production trap, a procedure that we named *direct injection*. We have demonstrated as of today the successful production of positronium inside of the trap apparatus using the *direct injection* and its excitation in-situ to Rydberg states.

The next milepost of the AE$\bar{g}$IS experiment will be to produce $\bar{H}$. Then the focus will shift toward further cooling of $\bar{p}$ with the aim of reaching temperatures well below 1 K, paramount to perform the high precision measurement, and onto the installation and commissioning of the deflectometer detector. Some of these operations will be delayed by the Long Shutdown 2 (LS2), a two year period spanning 2019 and 2020 after which the new stage of the decelerator, Elena, will be commissioned, which promises to deliver $\bar{p}$ at low enough energies to be captured directly by AE$\bar{g}$IS increasing considerably the system efficiency. At the same time the secondary chamber will continue to be available even across the LS2 and will be employed to further perform positronium spectroscopy, e.g.: by investigating the formation of long-lived $n = 2$ metastable states by spontaneous decay of $n = 3$ positronium.

4 Conclusions

The commissioning of the AE$\bar{g}$IS experiment is steadily progressing. Most of the apparatus has already been built and commissioned with the only major component still missing being the moiré deflectometer, a prototype of which has already been tested[3]. The apparatus has demonstrated its capabilities to manipulate antiprotons, positrons and positronium while, at the same time, providing the ability to perform direct investigation of positronium physics. In the current circumstances it is reasonable to expect production of $\bar{H}$ in the near future.

Acknowledgements

This research project has been supported by a Marie Skłodowska-Curie Innovative Training Network Fellowship of the European Commission's Horizon 2020 Programme under contract number 721559 AVA

References

[1] T. A. Wagner, S. Schlamminger, J. H. Gundlach, and E. G. Adelberger, Classical and Quantum Gravity, **29** 184002, (2012)
[2] ALPHA and A. E. Charman, Nature Communications, **4** 1785 (2013)
[3] S. Aghion et al. (AEGIS collaboration), Nature Comm. **5** 4538 (2014)
[4] D. Krasnický, R. Caravita, C. Canali, and G. Testera, Phys. Rev. A, **94** 022714 (2016)
[5] M. Amoretti et al, Nature **419** 456–459 (2002)
[6] Drobychev G et al, CERN-SPSC-2007-017 (2007), `http://cdsweb.cern.ch/record/1037532`

[7] S. Mariazzi, P. Bettotti, S. Larcheri, L. Toniutti, and R. S. Brusa, Phys. Rev. B **81** 235418 (2010)
[8] S. Mariazzi, P. Bettotti, and R. S. Brusa, Phys. Rev. Lett. **104** 243401 (2010)
[9] A.P. Mills, Jr, E.M. Gullikson, Appl. Phys. Lett. **49** 1121 (1986)
[10] T.J. Murphy, C.M. Surko, Phys. Rev. A **46** 5696 (1992)
[11] S. Cialdi, I. Boscolo, F. Castelli, F. Villa, G. Ferrari, M.G. Giammarchi, Nucl. Instrum. Methods B 269 1527 (2011)
[12] S. Aghion et al. (AEGIS collaboration), Nucl. Instrum. Methods B **362** 86 (2015)
[13] D. B. Cassidy, S. H. M. Deng, H. K. M. Tanaka, and A. P. Mills, Appl. Phys. Lett. **88** 194105 (2006)
[14] S. Aghion et al. (AEGIS collaboration), Phys. Rev. A **94** 012507 (2016)
[15] A. Deller, A. M. Alonso, B. S. Cooper, S. D. Hogan, and D. B. Cassidy, Phys. Rev. A **93** 062513 (2016)